Tellus SERIES A DYNAMIC METEOROLOGY AND OCEANOGRAPHY
PUBLISHED BY THE INTERNATIONAL METEOROLOGICAL INSTITUTE IN STOCKHOLM

Tellus (2009), 61A, 129–143
Printed in Singapore. All rights reserved

TELLUS

Inferred variables in data assimilation: quantifying sensitivity to inaccurate error statistics

By MARTIN JUCKES* and BRYAN LAWRENCE, *British Atmospheric Data Centre, Rutherford Appleton Laboratory, Chilton, Didcot, Oxon OX11 0QX, UK*

(Manuscript received 28 March 2008; in final form 30 September 2008)

ABSTRACT

The ability of data assimilation systems to infer unobserved variables has brought major benefits to atmospheric and oceanographic sciences. Information is transferred from observations to unobserved variables in two ways: through the temporal evolution of the predictive equations (either a forecast model or its adjoint) or through an error covariance matrix (or a parametrized approximation to the error covariance). Here, it is found that high frequency information tends to flow through the former route, low frequency through the latter. It is also noted that using the Kalman Filter analysis to estimate the correlation between the observed and unobserved variables can lead to a biased result because of an error correlation: this error correlation is absent when the Kalman Smoother is used.

1. Introduction

As observing systems become increasingly complex, involving many streams of information, the study of complex geophysical systems is increasingly carried out with the help of assimilation systems which filter, regularize and interpolate the data as necessary. This paper looks at one aspect of the assimilation process: the ability to infer the values of unobserved variables.

Juckes and Lawrence (2006) studied the random walk, in the context of both filtering and smoothing data analyses (Kalman and Bucy, 1961). Here an oscillatory system is studied in order to investigate the impact of different analysis systems on the accuracy of the inferred variables.

Studying a single mode allows us to derive explicit expressions for the error covariances. These solutions show how information is transferred to the unobserved variable both through the synthesis step and through the forecast step.

Polavarapu et al. (2005) draw attention to the detrimental impact of biases on scientific exploitation of reanalyses, in the context of the strength of the Brewer–Dobson circulation. This circulation is not observed, but inferred through the assimilation process. The possibly detrimental effects of artificial sources and sinks produced through the assimilation system have been widely discussed. The error covariances and the biases they induce in flux estimates are discussed below.

The factors affecting the accuracy of the analysis can be put into three main categories: the accuracy of the observation, accuracy of the model, and the accuracy of the error statistics. This paper also looks at the insensitivity of the analysis to model error covariance misspecification found in Sørensen et al. (2006), Juckes and Lawrence (2006) and Juckes (2006). Sørensen et al. (2006) present empirical evidence of this insensitivity: here a simple analytic model will be used to give explicit results.

The Kalman Filter and Kalman Smoother are used. The relation between these and other algorithms used in meteorological analyses is discussed in Li and Navon (2001), Fisher et al. (2005). Some of the practicalities of using a Kalman Smoother in a re-analysis context have been discussed by Cohn et al. (1994), Todling et al. (1998) and Zhu et al. (2003).

2. The simple harmonic oscillator

2.1. Equations

We will consider a linear harmonic oscillator subject to random forcing. The random forcing will be treated as unknown to the assimilation system. For this very simple system the error covariance of the Kalman Filter and Smoother can be calculated explicitly. The system is sufficiently complex to investigate an important aspect of data assimilation: the ability to infer unobserved variables. In the work below it will be assumed that one component of the two-component system is observed and the second is left to be inferred by the assimilation system.

The components of the oscillator, (u, v), evolve as follows:

$$\frac{\partial u}{\partial t} - \omega v = \varsigma_1 W_1 + \gamma_1, \tag{1a}$$

$$\frac{\partial v}{\partial t} + \omega u = \varsigma_2 W_2 + \gamma_2, \tag{1b}$$

*Corresponding author.
e-mail: m.n.juckes@rl.ac.uk
DOI: 10.1111/j.1600-0870.2008.00376.x

where ω is the frequency, $\varsigma_{1,2}$ and $\gamma_{1,2}$ are constants, and (W_1, W_2) are Wiener processes (e.g. Stark and Woods, 2002) with a correlation W_c:

$$E\left[\int_t^{t+\Delta t} W_i(\tau)\,\mathrm{d}\tau \int_t^{t+\Delta t} W_j(\tau)\,\mathrm{d}\tau\right] = \begin{cases}\Delta t, & i = j,\\ W_c\Delta t, & i \neq j,\end{cases} \quad (2)$$

where $E[.]$ denotes the expectation value. eq. (2) holds for any time interval $(t, t + \Delta t)$. The assimilation model is as Eq. (1) with the right-hand side set identically to zero: the terms $\varsigma_{1,2}$ and $\gamma_{1,2}$ terms are thus, from the perspective of the assimilation, model random error and bias terms, respectively.

Appendix C shows how eqs (1a,b) can be replaced without approximation by discrete equations. If $u_k = u(k\mathrm{d}t)$, $v_k = v(k\mathrm{d}t)$, then the discrete equations take the form:

$$\begin{pmatrix} u_k \\ v_k \end{pmatrix} - P\begin{pmatrix} u_{k-1} \\ v_{k-1} \end{pmatrix} = P^{1/2}\begin{pmatrix} \bar{e}_1 + \gamma_1 \\ \bar{e}_2 + \gamma_2 \end{pmatrix}, \quad (3)$$

where $\bar{e}_i$, $i = 1, 2$ are Gaussian random variables and

$$P = \begin{pmatrix} \cos[\omega\mathrm{d}t/2] & \sin[\omega\mathrm{d}t/2] \\ -\sin[\omega\mathrm{d}t/2] & \cos[\omega\mathrm{d}t/2] \end{pmatrix}. \quad (4)$$

The covariance of the $\bar{e}_i$, Q, is calculated in Appendix C: it is expressed without approximation in terms of the covariance of W_i, the time interval $\mathrm{d}t$, and the frequency ω (eqs C4–C6).

Optimal estimates of the state for given observations can now be obtained with the standard discrete Kalman filter and smoother. The relevant equations are given in Appendix A, along with a description of the notation.

To summarize the notation of the discretized problem: P is the process model, Q the process model error covariance, B is the forecast error covariance, and $\hat{B}$ is the analysis error covariance. B and $\hat{B}$ are used with subscripts f for the forward (i.e. normal) Kalman Filter, b for the backward Kalman Filter and s for the Kalman Smoother. Components of covariance matricies will be indicated by subscript pairs, with '1' and '2' corresponding to the observed and unobserved variables, respectively.

A full list of the symbols used is given in Table 1.

2.2. Scaling

Six parameters describe the system: 5 introduced above (ω, ς_1, ς_2, $\mathrm{d}t$ and W_c) plus the amplitude scale of the true solution, which we will denote U. These six parameters can be combined into five independent non-dimensional parameters representing process noise, signal to noise ratio, system frequency, the ratio between process noise in observed and unobserved variables and the correlation between the latter two noise terms:

$$e_A = \frac{\varsigma_1\varsigma_2\mathrm{d}t}{\sigma_o^2} = \frac{\sigma_p^2}{\sigma_o^2} \quad (5)$$

$$\delta_A = \frac{U^2}{\varsigma_1\varsigma_2\,\mathrm{d}t} = \frac{U^2}{\sigma_p^2} \quad (6)$$

$$\nu_A = \omega\,\mathrm{d}t \quad (7)$$

$$\gamma_A = \frac{\varsigma_1}{\varsigma_2} \quad (8)$$

and W_c, which is already non-dimensional. Here, $\sigma_p^2 = \sqrt{Q_{11}Q_{22}}$ is the geometric mean of the process model error variance. e_A is a measure of the model error relative to the observational error, δ_A is a measure of signal amplitude relative to the model noise, ν_A is the system frequency non-dimensionalized by the observation period, and γ_A is the ratio of modelling error in the observed variable to that in the unobserved variable.

It is also convenient to introduce a dependent non-dimensional variable,

$$\epsilon_A = \frac{e_A}{\nu_A} = \frac{\varsigma_1\varsigma_2}{\omega\sigma_o^2}, \quad (9)$$

where ϵ_A measures the ratio of the noise affecting the oscillator over over the timescale of an oscillation to the noise in the observations.

3. Preliminary results

3.1. Smoothness and error variance reduction

Figures 1 and 2 show the results of observing the simple system analysed with three assimilation techniques (the forward and backward Kalman filters and the Kalman smoother) and with different ratios of process noise to observational noise (e_A) and to signal amplitude (δ_A). In both figures, the two components in eq. (1) were equal and uncorrelated (i.e. $\varsigma_1 = \varsigma_2$ and $W_c = 0$), so that $Q = \sigma_p^2 I$, where I is the identity matrix. In each case, a realization of (u_k, v_k), $k = 1, ..N$, as defined by eq. (3) is constructed using pseudo-random numbers from the IDL random number generator. (u_0, v_0) are initialized to (4, 0) (and hence $U = 4$), the solution is generated with a time discretization of 0.1. See figure caption for other parameter details.

Pseudo observations of the u component are taken, again using pseudo-random noise to emulate observational errors:

$$y_k = u(k\,\mathrm{d}t) + e_o, \quad (10)$$

where the observational noise variance is $E[e_o^2] = \sigma_o^2, k = 1, ..N_{obs}$. Figures 1 and 2 show results for $\mathrm{d}t = 1$.

In Figs. 1 and 2 it can be seen that useful inference of the unobserved variable can be obtained even with very inaccurate observations ($\sigma_o \approx U$) and with a very inaccurate model ($\delta_A < 1$) (for the assimilation, both variables are initialized to zero, and would remain zero in the absence of any assimilation).

The discontinuities seen in the forward and backward Kalman filter analyses in Figs. 1 and 2 occur from the discontinuities in information content which occur every time a new observation is incorporated into the analysis. By contrast, the Kalman Smoother uses both future and past observations. It follows that

Table 1. Table showing notation used. Optional subscripts and superscripts are listed after the symbols in square brackets. For example, $[b|f|s]$ indicates that the symbol may take one of b, f or s in the indicated position

	Symbol	Description	First use
Operators	E	Expectation	eq. (2)
	$W_{[i]}$	Wiener process	eq. (1)
Matrices	P	Process model	eq. (3)
	$Q_{[k]}$	Process model error covariance	After eq. (3)
	$B^{[n]}_{[b\|f\|s][k]}$	Forecast error covariance	Section 2.1, Appendix A
	$\hat{B}^{[*\|\dagger][n]}_{[b\|f\|s][k]}$	Analysis error covariance	Section 2.1, Appendix A
	$\Gamma_{[b\|f\|s]}$	Bias sensitivity	eq. (15)
	K	Kalman gain	Appendix A
	H	Observation operator	Appendix A
	$R_{[k]}$	Observation error covariance	Appendix A
Vectors	$(u, v)_{[a\|k]}$	Variables in the simple harmonic oscillator	eq. (1)
	$(\varsigma_1, \varsigma_2)$	Amplitudes of noise in the simple harmonic oscillator	eq. (1)
	b	Bias in analysis	eqs (15, B8)
	$\overline{e}$	Random error in discrete model equations	eqs (3, C2)
	γ	Bias in model equations	eqs (1, B8)
Scalars	dt	Observation interval	eq. (4)
	k	Time interval index	eq. (3)
	A_{is}	Information asynchronicity	eq. (13)
	N_{obs}	Total number of observations	eq. (10)
	U	Scale of signal	Section 2.2
	$\mathcal{S}_{ij}$	Error sensitivity	eq. (14)
	c, s	$\cos(\omega dt)$, $\sin(\omega dt)$	Appendix D
	c_h, s_h	$\cos(\omega dt/2)$, $\sin(\omega dt/2)$	Appendix D
	t, τ	Time	eqs (1, 2)
	e_A	Model error integrated over observation interval, normalized by σ_o^2	eq. (5)
	δ_A	U^2 normalized by model error integrated over observation interval	eq. (6)
	ν_A	Observation interval times system frequency	eq. (7)
	γ_A	Ratio of observational error variance in observed to unobserved variable	eq. (8)
	$\sigma^{[\dagger]}_{[p\|o]}$	Error variance	Below eq. (8)
	ω	Frequency of SHO	eq. (1)
Subscripts	$b\|f\|s$	Backward/Forward Kalman Filter and Kalman Smoother	Appendix A
	$p\|o$	Process/Observational (applied to error variances)	
	i, j,1,2	Component index	
	a	Analysis	
	A	Non-dimensional scalar	
	h	See c_h, s_h under scalars	
	k	As under 'Scalars'	
Superscripts	$\dagger$	Denotes an estimated error statistic used as input to an assimilation, and the associated estimate of analysis or forecast error statistics	
	$*$	Denotes actual analysis or forecast error statistics in cases where incorrect input error statistics are used	
	n	Non-dimensionalized by σ_o^2	
	T	Transpose	

there are no discontinuities in the information content and hence no discontinuities in the optimal solution.

The Kalman smoother is a weighted linear combination of the forward and backward filters. Generally, this results in u_s lying between u_f and u_b, but not always. The weighting by the error covariances and the fact that both u and v components of the filters influence u_s can lead to a situation in which u_s lies outside of the range spanned by u_f and u_b. This occurs over roughly

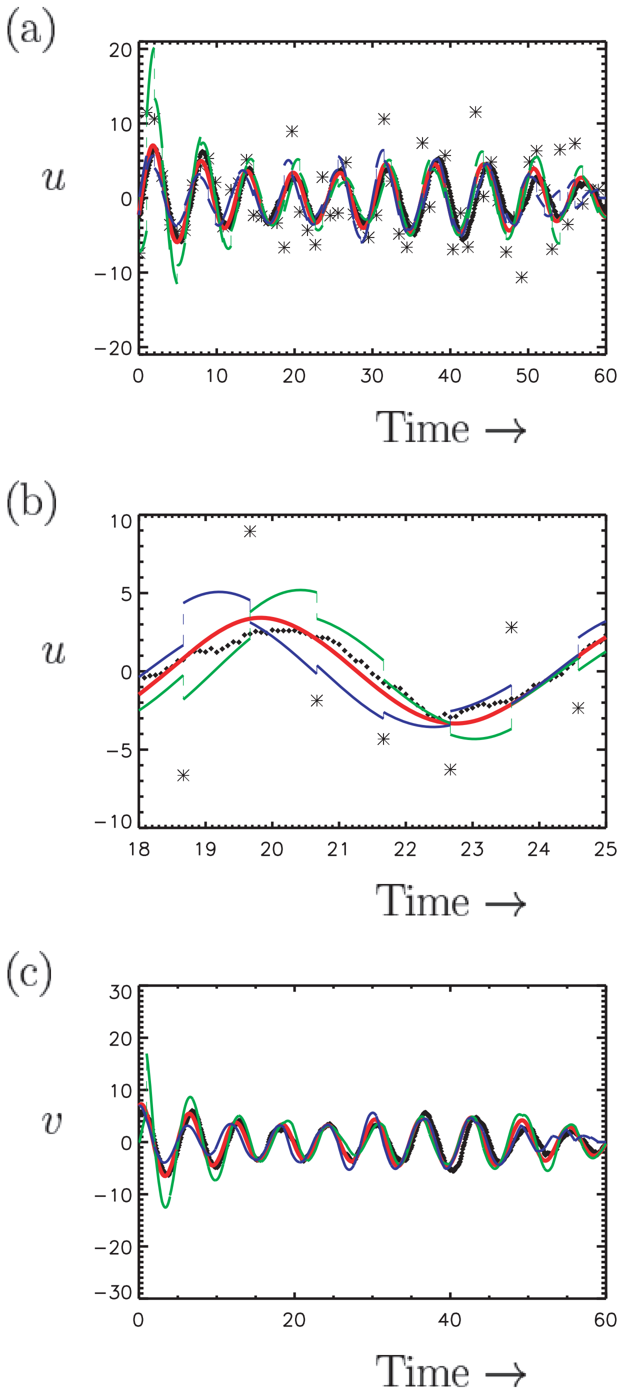

Fig. 1. Target trajectory and assimilation, $\nu_A = 1$, $e_A = 0.04$, $\delta_A = 16$, $\gamma_A = 1$, $W_c = 0$, $\omega = 1$ and $\sigma_o = 5$. (a) Simulated observations and u, (b) a magnified section of (a), and (c) inferred v from the assimilation. The forward solution of the equations is shown by black diamonds (which form a continuous line in this case), and the Kalman Filter, Backward Filter and Kalman smoother as green, blue and red lines respectively. Time, u and v are dimensionless.

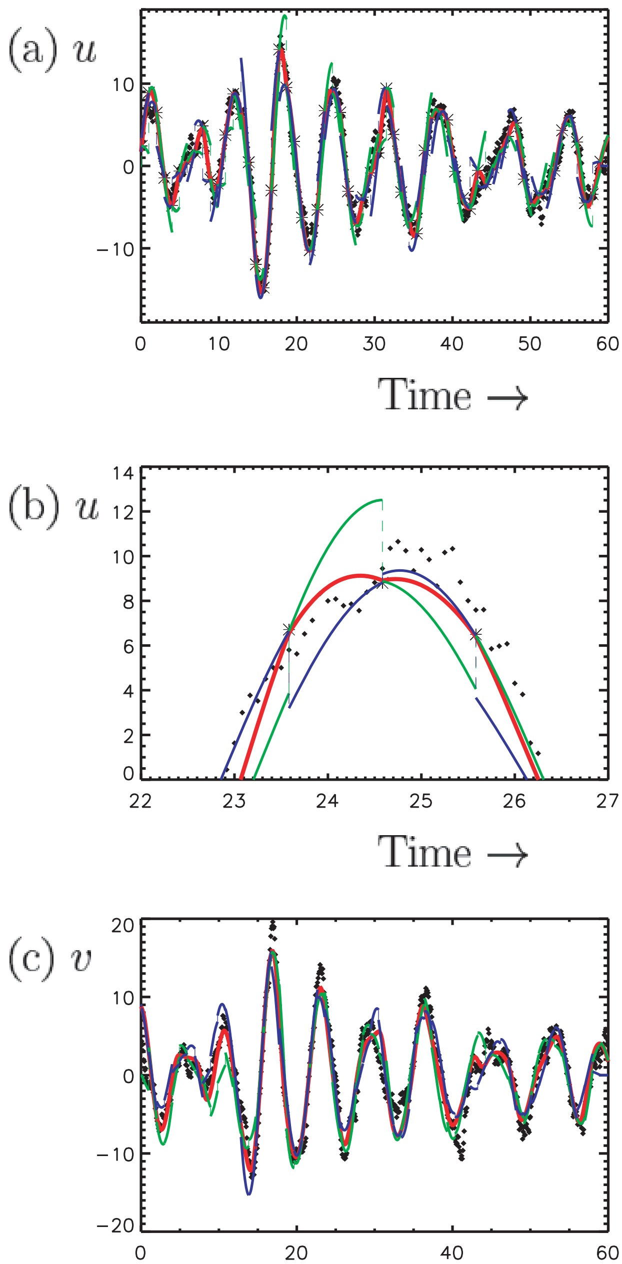

Fig. 2. As Fig. 1, except for $e_A = 25$, $\sigma_o = 1$, $\delta_A = 0.64$.

7% of the time interval for the solution shown in Fig. 1, but by amounts which are barely visible.

3.2. *Error covariances*

The information content can be understood by evaluating the analysis error covariance, $\hat{B}$. This can be calculated analytically if the observations are regularly spaced and have uniform error variance. The calculation is essentially the same as that carried out in Juckes and Lawrence (2006) for stable and unstable random walks, except that the scalar error variance there is replaced by a 2×2 error covariance matrix. If both components are observed the problem can easily be reduced to a scalar one, exploiting the symmetry between the two components. If only one component is observed the symmetry of the problem is broken leading to a set of coupled quadratic equations for the three independent components of the covariance matrix. This can be expressed as a discrete algebraic Riccati equation (e.g. Brogan, 1991) for the background error covariance, $\hat{B}$. Appendix D solves the problem for the simple harmonic oscillator by reducing it to a single quartic equation for $\hat{B}_{f11}$ and using a substitution which reduces the quartic to two quadratics, such that the solution of the first quadratic gives the coefficients of the second. While the solution is algebraically complex, it does give a complete description of the dependence of the non-dimensional error covariance, normalized by the observational error variance, on a 4 dimensional parameter space spanned by e_A, ν_A, γ_A and W_c (the error is independent of U).

Figure 3 shows, for the case of uncorrelated model errors ($Q_{12} = 0$: see Appendix C), the error covariance elements for the Kalman Filter, normalized by the observational error variance and displayed as functions of $\sin(\nu_A)$ and $\epsilon_A/(\epsilon_A + 1)$ (this coordinate for the x-axis is chosen so that the entire range $0 \leq \epsilon_A \leq \infty$ can be displayed on a finite axis running from 0 to 1). The y range only displays results down to an observing frequency of once per cycle. The general gradient from left- to right-hand side in all panels shows how increasing model error leads to increasing error in the analysis. In the case of the observed variable (Fig. 3a) this is, of course, limited by the error in the observations (the validation here is done at an observation time, larger errors will generally be found between observation times). The unobserved variable, on the other hand, has an error variance (Fig. 3b) which, for fixed observational error variance, increases without bound as the model error increases.

The variation from top to bottom of each figure shows the change in error covariance which would result from increasing the observing frequency. Increased observational frequency can reduce the error in the observed component to arbitrarily small values (Fig. 3a), but for the unobserved variable there is a finite limit dependent on ϵ_A (Fig. 3b). At small ϵ_A it can be shown that, for the Kalman filter, the error variance of the observed variable is given by

$$\hat{B}^n_{f11} \approx \begin{cases} 2\epsilon_A & e_A \ll 1, \nu_A, \\ \epsilon_A & \nu_A \lesssim \epsilon_A \ll 1. \end{cases}$$

Figure 3b shows that, as expected, $\hat{B}_{f22}$, the error variance in the inferred variable normalized by the observational error, increases without limit as the model noise variance increases (going from left- to right-hand side in the figure). For large model noise, $e_A \gg 1$, it can be shown that the analysis error variance for the inferred variable is related to the process model error covariance Q by:

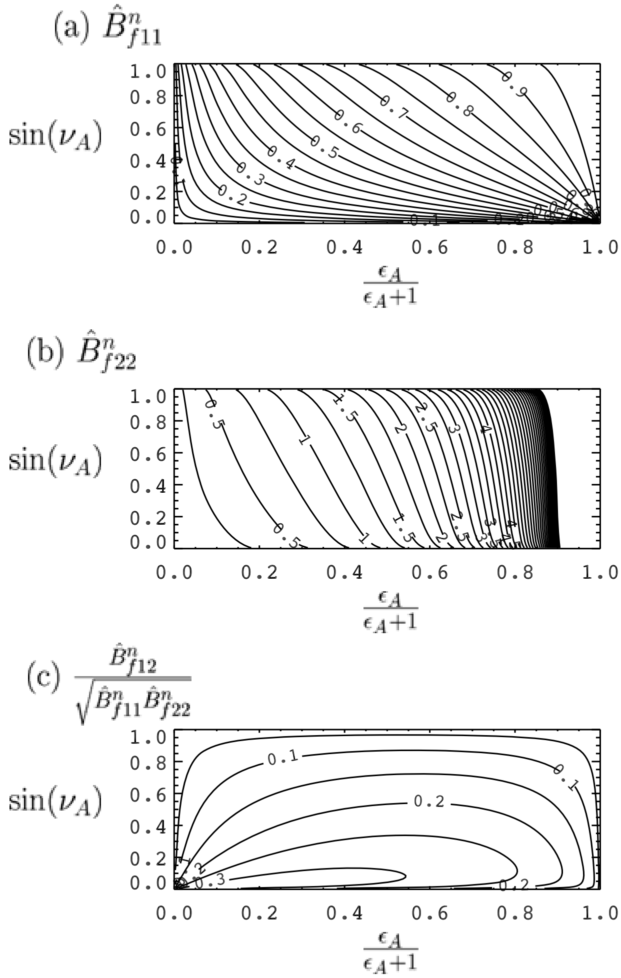

Fig. 3. Error covariances for Kalman filter applied to the simple harmonic oscillator. Component '1' is the observed variable (u), component '2' the inferred variable (v). (a) Observed variable analysis error variance, (b) unobserved variable analysis error variance, and (c) analysis error correlation between observed and unobserved variables. The x-axis scale is such that the entire range $0 < \epsilon_A < \infty$ is shown. Other parameters are $\gamma_A = 1$ and $W_c = 0$.

$$\hat{B}_{22} \approx \frac{1}{\sin(\nu_A)} \left(\sqrt{Q_{11} Q_{22}} - Q_{12} \right) \tag{11a}$$

$$(\nu_A > 0, \quad |Q_{11} Q_{22} - Q_{12}^2| \gg \sigma_o^2). \tag{11b}$$

The second of the above conditions excludes the singular case of near perfect correlation between the model error coefficients. As might be expected, this component of the error grows in proportion to the model noise variance.

The correlation between the analysis errors of the observed and unobserved variables, $\hat{B}^n_{f12}/\sqrt{\hat{B}^n_{f11}\hat{B}^n_{f22}}$, is shown in Fig. 3c. It maximizes at small ν_A, with a maximum value slightly over 0.327. The errors become uncorrelated both on the limit of

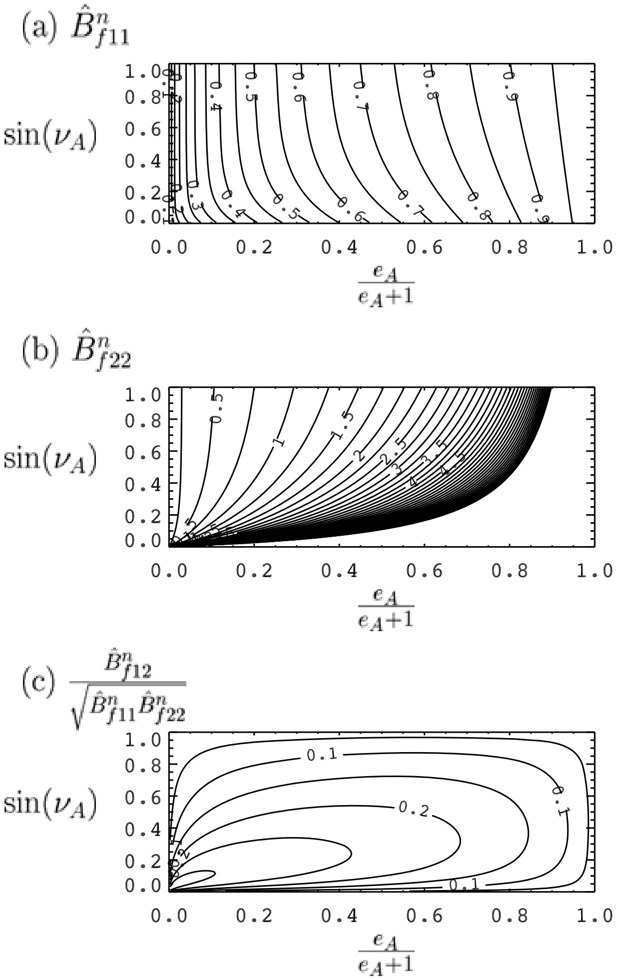

Fig. 4. As Fig. 3, except plotted against $e_A/(1+e_A)$.

$\epsilon_A \to 0$ (small model error) and $\epsilon_A \to \infty$ (large model error). The error correlation also vanishes when $\nu_A = \pi$, that is, when the observations are spaced at half the oscillators period. $\hat{B}_{12}$ is discussed further in Section (3.3) below.

Figure 4 shows the results plotted in Fig. 3, but now plotted on different axes so that the top to bottom gradient shows how the error covariance varies as a function of ω at fixed dt. The error variance in the inferred variable increases rapidly as $\omega \to 0$ as predicted above in the discussion of eq. (11a). Equation (11a) also suggests that the error in the inferred variable is large for low frequencies and frequent sampling ($\nu_A = \omega \mathrm{d}t$ small), provided that the model error correlation, $Q_{12}/\sqrt{Q_{11}Q_{22}}$ is not too close to unity. A strong error correlation leads to enhanced flow of information to the unobserved variable. This is slightly misleading because there is some cancellation between terms in this limit as Q is also dependent on these parameters (see Appendix C). Taking into account these factors, it can be shown that the small dt limit of eq. (D5c) is:

$$\hat{B}^n_{22} \approx \epsilon_A(1 - W_c), \quad \hat{B}_{22} \approx \varsigma_1\varsigma_2(1 - W_c)/\omega, \tag{12a}$$

$$(1 \gg \nu_A > 0, \quad |Q_{11}Q_{22} - Q_{12}| \gg \sigma_o^2). \tag{12b}$$

Thus, we have amplification of the error variance for ω small, and the error variance in the unobserved variable is independent of both σ_o and dt in this limit. That is, σ_o and dt have been reduced to the point where further changes make no difference: (12a) gives the minimum error which is obtained in the unobserved variable when observation of the observed variable is perfect.

Equation (11a) also shows that there is amplification of the $\hat{B}_{22}$ as $\omega \mathrm{d}t \to n\pi$ for any integer n; that is, there are large errors in the unobserved variable when the observing frequency is an integer multiple of half periods. This singularity occurs because the u and v equations are uncoupled when $\omega \mathrm{d}t = n\pi$. The assumption, used in Appendix C, that the Kalman Filter error covariances reach a steady limit is then not valid: the error variance in the unobserved variable grows linearly with time. Physically this is a result of the weak coupling between the two variables in this limit (recall that w is essentially a coupling parameter in this system), which means that the flow of information from the observed to the inferred variable will be weak. Equation (12a) shows that $\hat{B}_{22}$ is independent of dt as d$t \to 0$, so increasing the frequency of observations cannot reduce the analysis error variance of the unobserved variable below the limit set by eq. (12a). This result is likely to be relevant for wave-like modes in more complex systems, but it is not clear to what extent it will apply to other types of coupling.

Comparing Fig. 3b with Fig. 4b, it can be seen that the analysis error variance of the unobserved variable, $\hat{B}_{22}$, has a wide range of values for any given e_A, but varies over a relatively small range for any fixed ϵ_A. That is, the model error normalized by the system frequency is a better indicator of the unobserved variable error than the model error normalized by the observation interval. In order to obtain $\hat{B}_{22}$ comparable to the observation error covariance, for instance, a value of $\epsilon_A \approx 0.3$ is needed. In other words, when the accumulated model error over approximately one third of a period of the oscillator matches the observation error, we get an error in the unobserved variable comparable to the observation error.

As in Juckes and Lawrence (2006), these plots can be interpreted in terms of the influence of asynchronous observations on the analysis. The ratio of information in the observations to that in the analysis is now a matrix, so its amplitude is not uniquely defined. If, for simplicity, we take the L_∞ norm (the maximum of the row-sums of the matrix), then the analysis information asynchronicity as defined by Juckes and Lawrence (2006) is simply:

$$A_{is} \equiv \hat{B}^n_{f11}, \tag{13}$$

which was shown in Figs. 3a and 4a. As model skill increases (to the left-hand side of Figs. 3a and 4a) or as observational frequency increases (towards the bottom of Fig. 3a), A_{is} decreases, implying that the analysis is increasingly dominated by asynchronous observations.

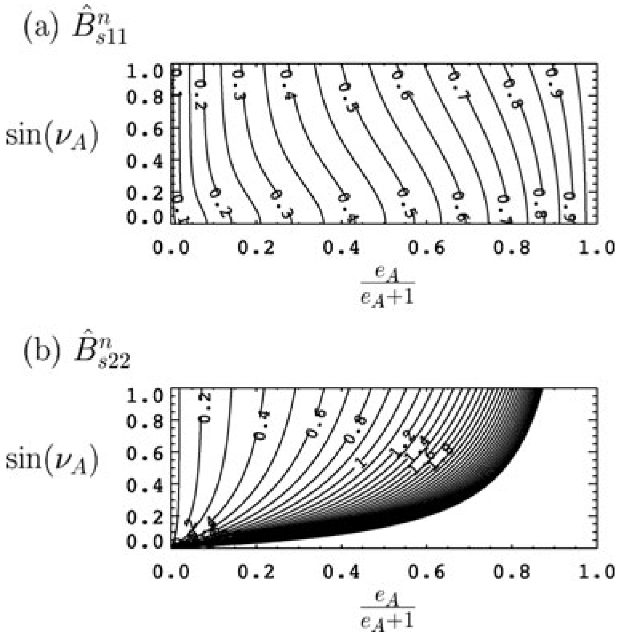

Fig. 5. As Fig. 3, except for the Kalman smoother, (a) observed variable analysis error variance and (b) unobserved variable analysis error variance.

Similar patterns are seen for the Kalman Smoother error variances (Fig. 5), except that the covariance term now vanishes identically (discussed further below). As is the case for the neutral random walk ($\alpha = 0$), described in Juckes and Lawrence (2006), the ratio of the error in the Smoother relative to that in the Filter approaches unity as the model skill decreases and approaches 0.5 as the observational skill decreases.

3.3. *Bias in derived fluxes*

In addition to the errors present in the assimilated and inferred variables, an important question is what influence these have on derived quantities. In the atmosphere important derived quantities include quadratic fluxes used to quantify a range of physical processes.

Evaluation of the analysis error matrix reveals a striking difference between the Kalman Filter and the Kalman Smoother. If $Q_{12} = 0$ and $Q_{11} = Q_{22}$, then the Kalman Smoother analysis error covariance vanishes identically (i.e. $\hat{B}_{s12} = 0$). This is a consequence of the symmetry of this problem with respect to time reversal, which depends in turn on (i) the system being linear with no explicit time dependence, (ii) evenly spaced observations, (iii) model and observation error statistics which have no time dependence and (iv) the harmonic coupling between the observed and unobserved variable. Under these conditions the error covariance of the backward filter can be obtained from that of the forward filter by reversing the sign of ω. Since the covariance term $\hat{B}_{f12}$ is proportional to $\sin \omega \mathrm{d}t$, it follows there is exact cancellation of the '12' terms in eq. (B5b). By contrast, the Kalman Filter produces error correlations (Fig. 3c) of up to 0.327. In other words, in the situation described here, unlike the Kalman Smoother, even using a perfect model and perfect statistical information the Kalman Filter produces analyses which have a bias in their covariances.

The impact of such biases will be particularly relevant to estimation of heat fluxes in atmospheric analyses. For example, in stratospheric analyses the temperature is measured and the wind field is normally inferred. There is therefore potential for significant error correlations to be generated: where analysis systems have time asymmetric assimilation components, even if the model itself were perfect, systematic biases would be present in the eddy fluxes of such analyses. This suggests that this could be a problem even in state-of-the art analyses, such as ERA40 (Uppala et al., 2006), which doesn't use a Kalman Filter, but does use a system which has the time asymmetry which generates the error correlation.

The expense of the standard Kalman Smoother algorithm has meant that the full algorithm is not generally considered as an option for large-scale problems. While this is not a problem for assimilation systems aimed at forecasting, Juckes and Lawrence discuss the advantages of the Kalman smoother for assimilations systems aimed at best estimation of state at some past time. We have shown here that biases in derived quantities are another reason why solutions based on the Kalman smoother are preferable for historical analyses. However, the Kalman smoother can be deployed in some large-scale problems: Juckes (2006, 2007) has demonstrated that a relaxation algorithm can derive the Kalman Smoother solution for assimilation with an isentropic advection model in a numerically efficient manner.

4. Sensitivity to incorrect error variance estimates

The Kalman Filter requires the model error covariance Q to be known. But how accurately does it need to be known? In numerical weather prediction applications it will not be possible to know all the details of Q. A similar problem occurs in the context of optimal interpolation (or kriging), in which case Stein (1997) has established bounds for the analysis errors resulting from a specific class of misspecifications in the observational error correlation function used.

Petersen and McFarlane (1994) and Dong and You (2006) exploit control theory techniques to develop stable filters when there are unknown, but bounded, uncertainties in the model error statistics. In these filters, the Kalman gain matrix, K, is replaced with the solution of an algebraic Riccati equation. Sangsuk-Iam and Bullock (1990) show the conditions under which misspecification of the model error covariance can lead to filter divergence. They also show that under or overestimates of the input error covariances will lead to under or overestimates, respectively, of the analysis error covariances. This section investigates the robustness of the results of the Kalman Filter and Kalman Smoother to misrepresentation of Q, assessing the sensitivity of the actual analysis error covariances to misspecification of the input error statistics. The difference between the estimated and actual error covariances analysed by Sangsuk-Iam and Bullock (1990) is, for small misspecifications, linearly dependent on the amplitude of the misspecification: here we will be looking at the quadratic difference between the actual error covariance and the optimal error covariances which would be achieved if the correct input covariances were used.

4.1. *Sensitivity to incorrect specification of Q*

This subsection looks at the importance of the difference between the correct error covariance, Q, of the model and the representation of that error covariance in the assimilation, which will be denoted $Q^\dagger$ here. In general, $Q^\dagger \neq Q$, and in many cases Q is unknown. In such cases there are more variants of the analysis error covariance: the symbol $\hat{B}$ will continue to be used for the error covariance of an analysis computed with the correct Q matrix. The actual error covariance in an analysis computed with $Q^\dagger$ which will be denoted $\hat{B}^*$. In addition there error covariance estimate delivered by the Kalman Filter and Smoother algorithm when they are applied using $Q^\dagger$: this algorithmic covariance will be denoted $\hat{B}^\dagger$. Appendix B.1 derives a generic equation relating the difference between $\hat{B}^*$ and $\hat{B}$, that is, the difference between the error covariance obtained and the theoretical optimal error covariance, to the difference between $Q^\dagger$ and Q.

Inserting the error covariances for the simple harmonic oscillator discussed above gives a set of three linear equations for the sensitivity of the three components of the analysis error covariance to this perturbation.

We first consider the case $Q^\dagger_{12} = Q_{12} \equiv 0$ and look at the variation of the analysis error as a function of the incorrect model error covariance used: $Q^\dagger$. Figure 6a shows the analysis error covariance of the observed variable ($\hat{B}_{f11}$) as a function for $\log_2[\sigma_p^{\dagger 2}/\sigma_p^2]$ for two sets of parameters, where $\sigma_p^{\dagger 2} = \sqrt{Q^\dagger_{11} Q^\dagger_{22}}$. Solutions of eq. (B2), which are correct for arbitrary $\sigma_p^\dagger$, are shown as solid lines, and of eq. (B4) (correct for small perturbations) as dashed lines. Also shown are results from large ensembles, in which the error covariances are directly evaluated. These serve as an independent check on the algebraic manipulations leading to the analytic solutions, as the former have become highly intricate by this stage.

For small perturbations the error covariances show a quadratic dependence on the perturbation amplitude. This means that a 5% overestimate of σ_p generates the same increase in analysis errors as a 5% underestimate. At larger perturbation amplitudes, however, strong asymmetry develops: a large underestimate in σ_p^2 has greater impact on the analysis accuracy than a large overestimate.

We now look at the importance of the model error covariance, Q_{12}. It can be seen directly from the results of Appendix D that $\hat{B}_{f11}$ and $\hat{B}_{f12}$ are completely independent of Q_{12}. It follows that the Kalman filter analysis, $(\hat{u}^*_f, \hat{v}^*_f)$, is independent of $Q^\dagger_{12}$. The value of the predicted analysis error covariance for the

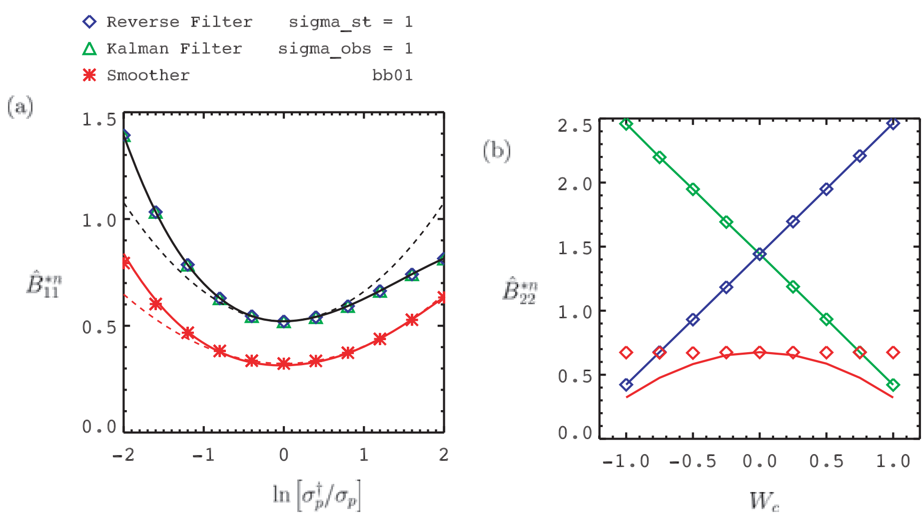

Fig. 6. The analysis error variance and the impact of (a) using an incorrect estimate of the model error variance (observed variable), (b) neglecting the model error covariance (unobserved variable). In (a) the analysis error covariance of the observed variable is shown, calculated using eq. B4 (black lines), the quadratic approximation (eq. B6, dashed lines): the lines are black for the Kalman filter and red for the Kalman smoother. In (b) the analysis error covariance of the unobserved variable is shown. The solid lines correspond to assimilations using the correct W_c, the symbols for assimilations completely neglecting W_c. Symbols are derived from an ensemble of numerical experiments: red stars: Kalman smoother; blue diamonds: backward filter; green triangles: Kalman filter. Other parameters are $\epsilon_A = 1$ and $\nu_A = 1$, and in (a) $W_c \equiv 0$, in (b) $\sigma^\dagger_p = \sigma_p$.

unobserved variable, $\hat{B}^{\dagger}_{f22}$, is, on the other hand, affected by $Q^{\dagger}_{12}$. The value of $\hat{B}^{\dagger}_{f22}$ has an impact on the Kalman Smoother estimate of the inferred variable, as shown in Fig. 6b. This can lead to situations in which the suboptimal Kalman Smoother is less accurate than the corresponding Kalman Filter, such as at the extreme right-hand side of Fig. 6b. With this set of parameters the Kalman Filter is much more accurate than the backward filter. If the algorithm uses a correlation of zero instead of 100% it will give the backward and forward solutions equal weight, thus degrading the solution by incorporating the greater error introduced by the backward filter. This is, however, an extreme case. For error correlations up to 50% the effect of neglecting them is minimal.

In Fig. 7 the sensitivity of the analyses to errors in σ_p^2 is presented using the following parameter:

$$\mathcal{S}_{ij} = \frac{\sigma_p^4 \delta \hat{B}_{ij}}{\hat{B}_{ij}\left(\sigma_p^{\dagger 2} - \sigma_p^2\right)^2}. \tag{14}$$

This is the relative increase in error normalized by the squared relative error in the assumed model error variance: it is the relevant measure of the sensitivity in the region where the quadratic approximation shown by the dashed line in Fig. (6a) is close to the full solution.

In all cases the sensitivity tends to zero as $e_A \to \infty$ and hence $e_A/(e_A + 1) \to 1$, that is, as the model noise in the observation interval becomes large compared to the observational noise. This simply reflects the fact that the analysis in this limit is equal to the observations and is unaffected by the value of Q. From Fig. 7 it can be seen that the low sensitivity seen in Fig. 6 is representative of the entire parameter range. Thus, large errors in the specification of the model error variance lead to a relatively modest degradation in analysis accuracy. This is consistent with the finding of Sørensen et al. (2006), in a study of reduced order Kalman filtering systems, that the accuracy of the assimilated fields are only significantly degraded by using 'extreme and unrealistic values' for the input error covariances.

The Kalman Smoother shows higher sensitivity than the Kalman filter over most of the parameter range displayed (shaded regions of Figs. 7d and e). In the inferred variable the Kalman Smoother always has lower sensitivity than the Kalman Filter. Lack of accuracy in the process error Q does not, however, alter the fact that the analysis error covariance term vanishes identically for the Kalman Smoother: if $B^*_f + B^*_b$, $\hat{B}_f + \hat{B}_b$ and $\hat{B}^{\dagger}_f + \hat{B}^{\dagger}_b$ are all diagonal then it follows that $B^*_f + B^*_b$ given by eq. (B5) is also diagonal.

4.2. Model bias

We now look at the effect of misspecification of the process model bias, γ_1, γ_2 in eqs (1,3). The preferred method of dealing with model bias in numerical weather prediction is by empirically estimating it and imposing a correction (e.g. Dee and

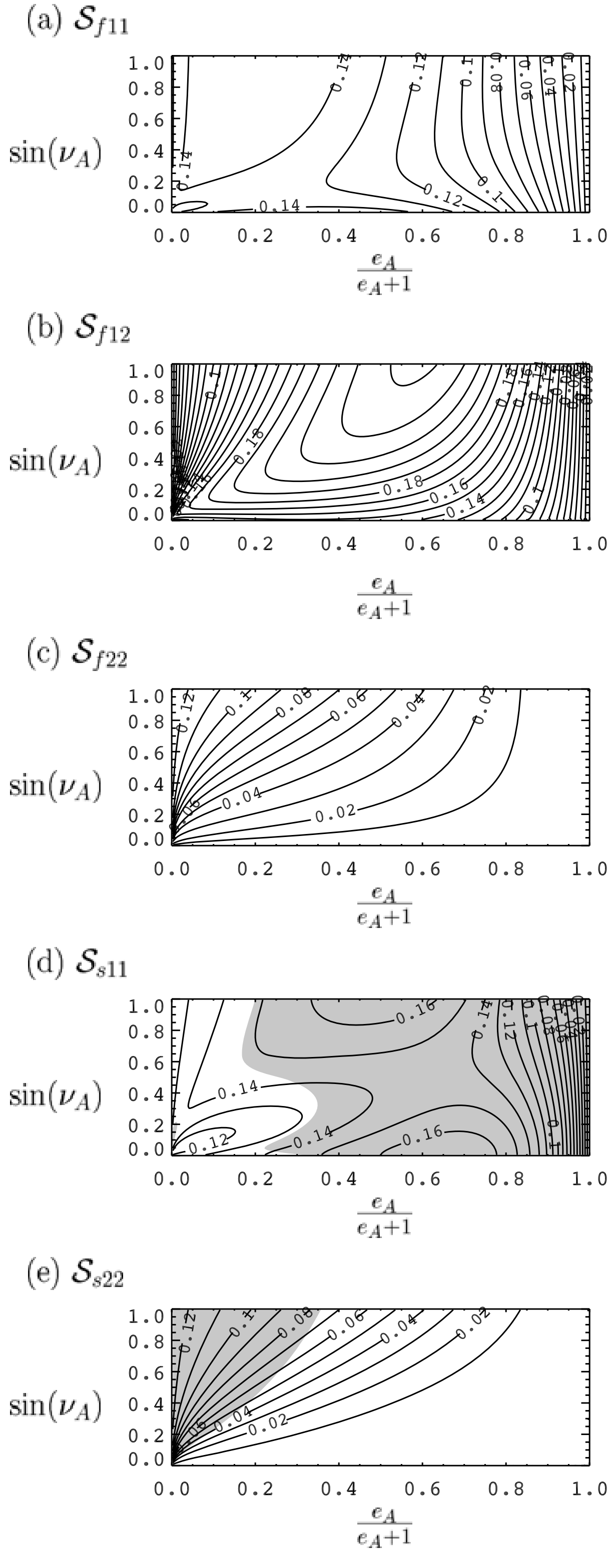

Fig. 7. Sensitivity of error covariances to inaccurate model error statistics. The x-axis is the relative error increase in error normalized by the squared relative error in the assumed model error variance. Other parameters are $\gamma_A = 1$ and $W_c = 0$.

Da Silva, 1998; Dee and Todling, 2000; Bell et al., 2004) or by refining the Kalman filter to provide a formal estimate of the bias (e.g. Keppenne et al., 2005; Gillijns and De Moor, 2006). The control theory work cited above (Sangsuk-Iam and Bullock, 1990; Petersen and McFarlane, 1994; Dong and You, 2006) has looked at what might be called first order model errors, in that the model P is equal to the true model plus an error P': here, as in the meteorological works cited in the previous sentence, we look at a zeroth order error, in that the increment over a time interval is given by $P\begin{pmatrix}u\\v\end{pmatrix}+\gamma$ and there is an error in γ. In this subsection we look at the impact of model bias on the analysis.

The bias in the solution is linearly related to bias in the forcing terms $\gamma_{u,v}$:

$$\begin{pmatrix}b_1\\b_2\end{pmatrix}=\Gamma\begin{pmatrix}\delta\gamma_u\\\delta\gamma_v\end{pmatrix}, \tag{15}$$

where Γ is a 2×2 matrix.

As outlined in the Appendix B, Γ can be evaluated, for the Kalman filter:

$$\Gamma_f=\frac{1}{\omega}\begin{bmatrix}0 & \frac{2(1-c)\left(\sigma_o^2-\hat{B}_{f11}\right)}{d_1}\\ 1 & \frac{\hat{B}_{f11}s-\hat{B}_{f12}(1-c)}{d_1}\end{bmatrix}, \tag{16}$$

where

$$d_1=\left(2\sigma_o^2-\hat{B}_{f11}\right)(1-c)+\hat{B}_{f12}s \tag{17a}$$

$$s=\sin\omega\,\mathrm{d}t \tag{17b}$$

$$c=\cos\omega\,\mathrm{d}t, \tag{17c}$$

For the Kalman Smoother

$$\Gamma_s=\begin{bmatrix}0 & \frac{2\hat{B}_{s11}\left(\hat{B}_{f22}\Gamma_{f12}+\hat{B}_{f12}\Gamma_{f22}\right)}{\hat{B}_{f11}\hat{B}_{f22}-\hat{B}_{f12}^2}\\ \omega^{-1} & 0\end{bmatrix}. \tag{18}$$

The non-trivial elements of the matricies $\Gamma_{f,s}$ are displayed in Fig. 8. Both Γ_{f21} and Γ_{f22} are singular as $\omega\to 0$. Thus, any bias in the system will produce large errors in the unobserved variable. When the Kalman smoother is used, $\Gamma_{s21}\equiv\Gamma_{f21}$, but Γ_{s22} vanishes. This means that a bias in the v equation will only produce a response in the u component of the analysis, and this response is bounded in the low frequency limit. Hence the problem of the low frequency singularity is eliminated from one component of the system, but remains in the other.

The sensitivity of the analysis of low frequency modes to bias in the model can be traced to the singularity of the matrix $(I-\hat{B}_f B_f^{-1}P)$ (see eq. B7A). The same matrix occurs in the expression for the impact of an observational bias, so the same sensitivity occurs.

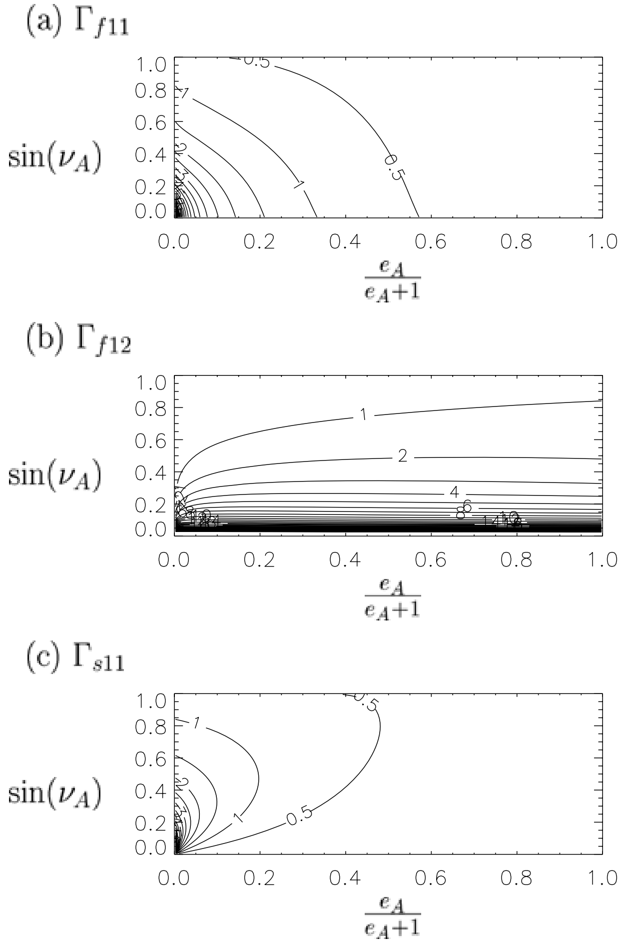

Fig. 8. Sensitivity of analysis bias to model bias. Other parameters are $\gamma_A=1$ and $W_c=0$.

5. Neglecting the background error covariance

In the Kalman Filter, information from the observations of u is transferred to the analysis estimate of v through two routes: (1) by the evolution of the model in the forecast step and (2) by projection in the synthesis step. The relative importance of these two routes can be illustrated by setting $B_{12}\equiv 0$ and thus cutting route (2) for the transfer of information from u to v. Appendix E gives optimal $\hat{B}^*_{11}$, $\hat{B}^*_{22}$, which deliver the best possible solution subject to the neglect of B_{12}. In a practical application these might be derived by tuning the assimilation system, but here they can be derived explicitly from the prescribed noise statistics.

The impact on $\hat{B}^\dagger_{11}$, where $\hat{B}^\dagger$ is the actual error covariance in the analysis, is small, with a maximum increase of 33.2%.

The ratio $\hat{B}_{22}/\hat{B}^\dagger_{22}$ is plotted in Fig. 9. The impact of neglecting B_{12} is small when $s=\sin(\omega\mathrm{d}t)$ approaches unity. In this parameter regime it appears that the information is transferred primarily through the model equations in the forecast step.

As s is reduced, however, the neglect of B_{12} causes increasingly severe degradation. This suggests that the information

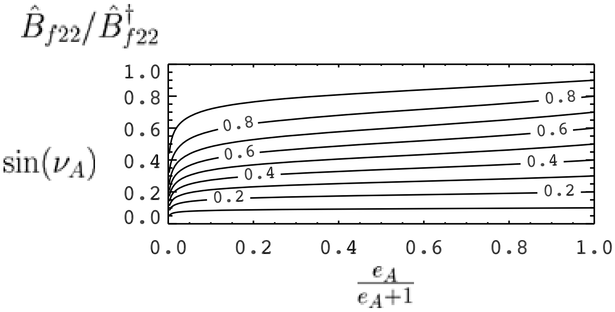

Fig. 9. Ratio of optimal error covariance in unobserved variable to suboptimal, both with the Kalman Filter, where the suboptimal solution is obtained neglecting the error covariance between the two components.

transfer through the model evolution is relatively weak, and hence that the dominant route for information transfer in the low frequency limit is through projection in the synthesis step.

Neglecting the off-diagonal terms in $\hat{B}$ is analogous to the approach used in the NOAA Rapid Update Cycle (RUC) (Benjamin et al., 2004) system, which inserts observations continuously without taking error covariances into account. The above calculation suggests that the RUC will produce near optimal results for high frequency modes, but may be deficient in low frequency modes, since the latter have small ν_A (this analysis neglects transfer between modes by non-linear interactions).

Snyder and Zhang (2003) and Zhang et al. (2004) discuss the ability of the Ensemble Kalman filter (ENKF) to transfer information to an unobserved variable. In their application they find that the covariance terms are important, and that the low order approximation to the covariance provided by the ENKF approach gives significant benefits.

6. Discussion

The properties of the Kalman Filter and Smoother when applied to a simple harmonic oscillator have been analysed, with observations taken only from one component of the oscillator.

Surprisingly, neglecting the model error covariance term Q_{12} has absolutely no impact on the accuracy of the Kalman Filter, though it does make the associated error variance estimates incorrect. This leads to an error in the Kalman Smoother solution, and, if the neglected error covariance is sufficiently large, to the smoother being less accurate than the filter.

If, on the other hand, the covariance term of the background error, B_{f12}, in the filter is neglected, there is a significant impact, especially at low frequencies, even when the remaining components of B_f are chosen to give the best possible results. At higher frequencies, on the other hand, neglect of B_{f12} has less significant impact.

It is found that the Kalman filter generates a spurious correlation between observed and unobserved variables in the analysis. The bias in the covariances is introduced by the time asymmetry in the Kalman Filter. This may have implications for the interpretation reanalyses such as the widely used 'ERA40' (Uppala et al., 2006) which share this time asymmetry.

Results of Section 5 suggest that an approach which neglects background error covariances and has frequent data input can work well for some components of the flow. The largest deficiencies are expected to be in the low frequency component.

7. Acknowledgments

This work was funded by NERC through the BADC Service Line Agreement.

8. Appendix A: The Kalman filter and Smoother

The Kalman filter equations are as follows:

$$x_{fk} = P\hat{x}_{fk-1}, \tag{A1a}$$

$$B_{fk} = P\hat{B}_{fk-1}P^T + P^{1/2}Q_kP^{1/2\,T}, \tag{A1b}$$

$$\hat{x}_{fk} = x_{fk} + K(y_k - Hx_{fk}), \tag{A1c}$$

$$\hat{B}_{fk} = (I - KH)\,B_{fk}, \tag{A1d}$$

$$K = B_{fk}H^T\left(HB_{fk}H^T + R_k\right)^{-1}, \tag{A1e}$$

(Kalman and Bucy, 1961). Subscripts f, b and s will be used to indicate the Kalman filter, backward filter and smoother respectively. A subscript k, $k \pm 1$ will be used to label the time interval. Following standard notation, Q is the noise covariance matrix, H the observation operator and R the observation error covariance. B will be the analysis error covariance. The state estimate x and error covariance B at any time level are written with a hat, '^', if they include observations from the current time level, otherwise these quantities refer to estimates which do not use the current observations. A 'T' superscript indicates a transpose.

The k subscript is omitted from H and K because for these operators the time is clear from the terms they are associated with. An algebraically more simple form of (A1c,d) is:

$$\hat{B}_{*k}^{-1}\hat{x}_{*k} = B_{*k}^{-1}x_{*k} + H^TR_k^{-1}y_k \tag{A2a}$$

$$\hat{B}_{*k}^{-1} = B_{*k}^{-1} + H^TR_k^{-1}H, \tag{A2b}$$

where the $*$ in the subscript can be f, b or s. Eqs (A1c,d) are preferred in numerical applications if the rank of R is less than the rank of B. The set (A1) avoids inversion of B, which is an enormous saving in many instances. The analytic manipulations in Appendix C will, however, start from the simpler form (A2).

Similar equations apply for the backward filter, simply replacing P with P^{-1}, and appropriate changes in indexing:

$$x_{bk} = P^{-1}\hat{x}_{bk+1} \tag{A3a}$$

$$B_{bk} = P^{-1}\hat{B}_{bk+1}P^{-1^T} + P^{-1/2}Q_{k+1}P^{-1/2^T} \tag{A3b}$$

along with the general expressions in eq. (A2). There is a subtlety in eq. (A3a): in order for this to be valid, the model noise in the interval $(k, k+1)$, $\overline{\epsilon}_k$, should be independent of $\hat{x}_{bk+1}$. However, is is clear that, for any given x_k, there will be a correlation between x_{k+1} and $\overline{\epsilon}_k$. The optimal estimates, $\hat{x}_k$ etc., are conditional and this conditionality creates conditional independence: just as the conditional probability of x_{k+1} give x_k, $Pr(x_{k+1}\,|x_k)$, is independent of $\overline{\epsilon}_{k-1}$, $Pr(\hat{x}_{k+1}|y_{k+1})$ is independent of $\overline{\epsilon}_k$. The conditional independence results from the fact that $\overline{\epsilon}_k$ influences $\hat{x}_{k+1}$ only through y_{k+1}.

The Kalman smoother is then:

$$\hat{x}_{sk} = \hat{B}_{sk}\left(B_{fk}^{-1}x_{fk} + B_{bk}^{-1}x_{bk} + H^T R_k^{-1} y_k\right) \tag{A4a}$$

$$\hat{B}_{sk}^{-1} = B_{fk}^{-1} + B_{bk}^{-1} + H^T R_k^{-1} H \tag{A4b}$$

9. Appendix B: Error evolution with imperfect models and error statistics

B.1. Random error

If the deterministic model is not correct there will be both a random and a deterministic component of the analysis error. We first look at the random component.

If $B_f^\dagger$ and $\hat{B}_f^\dagger$ are the estimated/empirical/erroneous error covariances used in the Kalman filter, possibly derived from less than perfect estimates, $P^\dagger$, $Q^\dagger$, of P and Q, then the random component of the error, B^*, evolves according to:

$$B_{k+1}^* = P\hat{B}_k^* P^T + P^{1/2}QP^{1/2\,T} \tag{B1a}$$

$$\hat{B}_{k+1}^* = \hat{B}_f^\dagger B_f^{\dagger^{-1}} B_{k+1}^* \left(\hat{B}_f^\dagger B_f^{\dagger^{-1}}\right)^T + \hat{B}_f^\dagger H^T R^{-1} H \hat{B}_f^{\dagger\,T}. \tag{B1b}$$

A more general version of this formula, allowing for errors in the observing operator H and the predictive model P was given by Heffes (1966), Griffin and Sage (1969).[1] If we assume a steady state, so that the error covariance at time k is the same as that at time k+1, eqs (B1a,b) can be rewritten as:

$$B_f^\dagger \hat{B}_f^{\dagger-1}\hat{B}_f^* \left(B_f^\dagger \hat{B}_f^{\dagger-1}\right)^T - P\hat{B}_f^* P^T = P^{1/2}QP^{1/2\,T} + B_f^\dagger H^T R^{-1} H B_f^{\dagger^T}. \tag{B2}$$

The optimal error covariances B, $\hat{B}$, which would be obtained using the deterministically perfect model an accurate error statistics, satisfy (B2) with $*$ and $\dagger$ superscripts removed. Subtracting this equation for the optimal solution from the (B2) gives an equation for the difference between the actual an the optimal error covariance as a function of the difference between the estimated and the optimal. If we assume that $B^\dagger$ and $\hat{B}^\dagger$ are consistent in the sense that:

$$\hat{B}_f^{\dagger-1} = B_f^{\dagger-1} + H^T R^{-1} H \tag{B3a}$$

$$\hat{B}_s^{\dagger-1} = \hat{B}_f^{\dagger-1} + \hat{B}_b^{\dagger-1} - H^T R^{-1} H. \tag{B3b}$$

Then:

$$\left(I + B_f H^T R^{-1} H\right)\left(\hat{B}_f^* - \hat{B}_f\right)\left(I + B_f H^T R^{-1} H\right)^T - P\left(\hat{B}_f^* - \hat{B}_f\right)P^T \approx \left(B_f^\dagger - B\right) H^T R^{-1} H \left(I - \hat{B}_f H^T R^{-1} H\right)\left(B_f^\dagger - B\right)^T, \tag{B4}$$

where terms in which $B_f^\dagger - B_f$ multiplies $\hat{B}_f^* - \hat{B}_f$ have been omitted.

The difference terms on the right-hand side, $B_f^\dagger - B$ and its adjoint vary linearly with changes in $Q^\dagger$ when the perturbation from Q is small. This shows that the actual error variance varies quadratically with the perturbation.

$$\hat{B}_s^* - \hat{B}_s = \hat{B}_s\left[\hat{B}_f^{-1}\left(B_f^* - B_f\right)\hat{B}_f^{-1} + \hat{B}_b^{-1}\left(B_b^* - B_b\right)\hat{B}_b^{-1}\right]\hat{B}_s \tag{B5a}$$

$$+\left(\hat{B}_s^\dagger \hat{B}_f^{\dagger-1} - \hat{B}_s\hat{B}_f{}^{-1}\right)\hat{B}_f\left(\hat{B}_s^\dagger \hat{B}_f^{\dagger-1} - \hat{B}_s\hat{B}_f{}^{-1}\right)^T \tag{B5b}$$

$$+\left(\hat{B}_s^\dagger \hat{B}_b^{\dagger-1} - \hat{B}_s\hat{B}_b{}^{-1}\right)\hat{B}_b\left(\hat{B}_s^\dagger \hat{B}_b^{\dagger-1} - \hat{B}_s\hat{B}_b{}^{-1}\right)^T \tag{B5c}$$

$$+\left(\hat{B}_s^\dagger - \hat{B}_s\right)H^T R^{-1} H\left(\hat{B}_s^\dagger - \hat{B}_s\right)^T \tag{B5d}$$

This gives a combination of the errors in the forward and backward components and an additional error due to the inaccurate combination of the two.

B.2. bias

Since the equation system is linear, the bias evolves independently of the solution and the random error. The amplitude of the bias in the solution results from the competition between the generation of bias by the forward model and the removal of bias by the addition of unbiased observations.

$$b_{fk+1} = P\hat{b}_{fk} + \gamma' \tag{B6a}$$

$$\hat{b}_{fk+1} = \hat{B}_f B_f^{-1} b_{fk+1} + K\delta y, \tag{B6b}$$

where δy is the bias in the observations.

If $\hat{b}_{fk+1} = \hat{b}_{fk} \equiv \hat{b_f}$ then

$$\hat{b}_f = \left(I - \hat{B}_f B_f^{-1} P\right)^{-1}\left(\hat{B}_f B_f^{-1}\gamma' + K\delta y\right), \tag{B7a}$$

$$\hat{b}_b = -\left(B_b\hat{B}_b^{-1} - P^{-1}\right)^{-1}\left(\hat{B}_b B_b^{-1}\delta\Gamma_b + K_b\delta y\right), \tag{B7b}$$

[1] Griffin and Sage calculate linear sensitivities: for the error covariance this vanishes identically and it is the quadratic sensitivity which is of interest.

$$\hat{b}_s = \hat{B}_s \left(\hat{B}_f^{-1}\hat{b_f} + \hat{B}_b^{-1}\hat{b_b} \right). \tag{B7c}$$

Where

$$\gamma' = -\frac{1}{\omega}\begin{pmatrix} s & 1-c \\ c-1 & s \end{pmatrix}\gamma \tag{B8}$$

is the integral of the bias over the interval dt, $\delta\Gamma_b$ is the same with the sign of s reversed, and K_b is the Kalman gain matrix for the backward filter.

10. Appendix C: Analytic integration of the random oscillator

Analytic integration of an unforced harmonic oscillator is trivial: this appendix shows how to extend the calculation to include the random term. Introduce the complex variable $z = u + iv$, so that

$$** \frac{\partial z}{\partial t} + i\omega z = W \overset{\text{def}}{=} \varsigma_1 W_1 + i\varsigma_2 W_2. \tag{C1}$$

This can then be integrated, without approximation, to give

$$z(t + \mathrm{d}t) = z(t)\exp(-i\omega \mathrm{d}t) + \overline{e}\exp(-i\omega \mathrm{d}t/2), \tag{C2}$$

where

$$\overline{e} = \int_t^{t+\mathrm{d}t} W(\tau)\exp\left[i\omega(\tau - d - \mathrm{d}t/2)\right]\mathrm{d}\tau. \tag{C3}$$

The covariance properties of $(\overline{e_1}, \overline{e_2}) = (\Re[\overline{e}], \Im[\overline{e}])$ now need to be determined.

It follows from the definition of the Wiener processes $W_{1,2}$ that

$$\begin{aligned} Q_{11} &= E[(\overline{e_1})^2] = E\left[\int_t^{t+\mathrm{d}t}\int_t^{t+\mathrm{d}t}\right. \\ &\quad \left\{\varsigma_1^2 W_1(\tau)W_1(\tau')\cos\phi\cos\phi'\right. \\ &\quad + \varsigma_1\varsigma_2 2W_1(\tau)W_2(\tau')\sin\phi\cos\phi' \\ &\quad \left.\left. + \varsigma_2^2 W_2(\tau)W_2(\tau')\sin\phi\sin\phi'\right\}\mathrm{d}\tau\mathrm{d}\tau'\right] \\ &= \omega^{-1}\int_{\omega\mathrm{d}t/2}^{\omega\mathrm{d}t/2}\left[\varsigma_1^2\cos^2\phi + \varsigma_2^2\sin^2\phi + W_{\mathrm{cor}}\varsigma_1\varsigma_2\sin 2\phi\right]\mathrm{d}\phi \\ &= \varsigma_1^2\mathrm{d}t + \frac{1}{2}\left(\varsigma_2^2 - \varsigma_1^2\right)\left(\mathrm{d}t - \frac{\sin\omega\mathrm{d}t}{\omega}\right), \end{aligned} \tag{C4}$$

where $\phi = \omega(\tau - t - \mathrm{d}t/2)$ and $\phi' = \omega(\tau' - t - \mathrm{d}t/2)$. Similarly,

$$Q_{22} = \varsigma_2^2\mathrm{d}t + \frac{1}{2}\left(\varsigma_1^2 - \varsigma_2^2\right)\left(\mathrm{d}t - \frac{\sin\omega\mathrm{d}t}{\omega}\right) \tag{C5}$$

and

$$\begin{aligned} Q_{12} &= E\left[\overline{e_1}\,\overline{e_2}\right] = 2\int_t^{t+\mathrm{d}t}\int_t^{t+\mathrm{d}t} \\ &\quad \left\{\left[\varsigma_1^2 W_1(\tau)W_1(\tau') - \varsigma_2^2 W_2(\tau)W_2(\tau')\right]\cos\phi\sin\phi'\right. \\ &\quad \left. + \varsigma_1\varsigma_2 W_1(\tau)W_2(\tau')\cos(\phi + \phi')\right\}\mathrm{d}\tau\mathrm{d}\tau' \\ &= W_{\mathrm{cor}}\varsigma_1\varsigma_2\frac{\sin\omega\mathrm{d}t}{\omega} \end{aligned} \tag{C6}$$

11. Appendix D: Evaluating analysis error covariances

If the observations are evenly spaced and have equal error covariance it is possible to derive an analytic expression for the error covariances of the Kalman filter and Smoother.

In this situation, the error variances converge towards a steady state which is independent of the time index, k (unless the problem is underdetermined, in which case the undetermined component of B grows without limit). If B is eliminated from (A1b) and (A2b), and the time index is dropped, we obtain the following equation for the steady state:

$$(\hat{B}^{-1} - H^T R^{-1} H)^{-1} = P\hat{B}P^T + Q',$$

where

$$Q' = P^{1/2} Q P^{T1/2}.$$

After some manipulation, the three components of this equation are:

$$\begin{aligned} \sigma_o^2\hat{B}_{11} &= \left(\sigma_o^2 - \hat{B}_{11}\right) \\ &\quad \times\left[c^2\hat{B}_{11} + s^2\hat{B}_{22} + 2cs\hat{B}_{12} + Q'_{11}\right] \end{aligned} \tag{D1a}$$

$$\begin{aligned} \sigma_o^2\hat{B}_{12} &= \left(\sigma_o^2 - \hat{B}_{11}\right) \\ &\quad \times\left[cs(\hat{B}_{22} - \hat{B}_{11}) + (c^2 - s^2)\hat{B}_{12} + Q'_{12}\right] \end{aligned} \tag{D1b}$$

$$\begin{aligned} \sigma_o^2\hat{B}_{22} - \hat{B}_{11}\hat{B}_{22} + \hat{B}_{12}^2 &= \left(\sigma_o^2 - \hat{B}_{11}\right) \\ &\quad \times\left[c^2\hat{B}_{22} + s^2\hat{B}_{11} - 2cs\hat{B}_{12} + Q'_{22}\right], \end{aligned} \tag{D1c}$$

where

$$c = \cos(\omega\mathrm{d}t), \quad s = \sin(\omega\mathrm{d}t). \tag{D2}$$

Eliminating $\hat{B}_{12}$ and $\hat{B}_{22}$ from eq. (D1) leads to a quartic equation for $\hat{B}_{11}$:

$$\begin{aligned} &s^2\left(2\sigma_o^2 - \hat{B}_{11}\right)^2\left[\left(\sigma_o^2 - \hat{B}_{11}\right)\left(Q'_{11} + Q'_{22}\right) - \hat{B}_{11}^2\right] \\ &\quad - \left[\left(\sigma_o^2 - \hat{B}_{11}\right)\left(cQ'_{11} - sQ'_{12}\right) - c\hat{B}_{11}^2\right]^2 = 0. \end{aligned}$$

Letting $z = \hat{B}_{11}^2/\left(\sigma_o^2 - \hat{B}_{11}\right)$ and dividing through by $\left(\sigma_o^2 - \hat{B}_{11}\right)^2$ reduces the quartic to a quadratic equation for z:

$$z^2 + 2b_z z + c_z = 0, \quad z = -b_z \pm \sqrt{b_z^2 - c_z}, \tag{D3}$$

where the coefficients are given by:

$$b_z = 2s^2\sigma_o^2 - \frac{1}{2}(Q_{11} + Q_{22}) - \frac{c}{2}(Q_{11} - Q_{22}) \tag{D4a}$$

$$c_z = -4\sigma_o^2 s^2\left(Q_{11} + Q_{22}\right) + \left(c_h^2 Q_{11} - s_h^2 Q_{22}\right)^2, \tag{D4b}$$

where $c_h = \cos(\omega\mathrm{d}t/2)$, $s_h = \sin(\omega\mathrm{d}t/2)$ The sign of the solution in eq. (D3) will be determined below.

Once z is known, $\hat{B}_{11}$ is determined from the definition of z, which can be rewritten as a quadratic equation for $\hat{B}_{11}$. The choice of root is determined by the fact that $\hat{B}_{11}$ must be positive. Hence, whatever the value of z:

$$\hat{B}_{11} = \frac{1}{2}\left(-z + \sqrt{z^2 + 4\sigma_o^2 z}\right), \tag{D5a}$$

$$\hat{B}_{12} = \frac{1}{2s}\left(1 - \sqrt{\frac{z}{z + 4\sigma_o^2}}\right)\left[cz - c_h^2 Q_{11} + s_h^2 Q_{22}\right] \tag{D5b}$$

$$\hat{B}_{22} = \hat{B}_{11} + \frac{1}{c}\left(1 + \frac{c^2}{s^2}\sqrt{\frac{z}{z + 4\sigma_o^2}}\right) \times \left[cz - c_h^2 Q_{11} + s_h^2 Q_{22}\right] - \frac{Q'_{12}}{cs}. \tag{D5c}$$

There are still two possible solutions, corresponding to the two possible value of z. It is found, however, that taking the negative root in eq. (D3) always produces either $z < 0$ or $\hat{B}_{11}\hat{B}_{22} - \hat{B}_{12}^2 < 0$ (determined by numerical evaluation): real solutions must have both these quantities positive, so it is the positive root in eq. (D3) which leads to the valid solution.

12. Appendix E: neglecting model error covariances

In large systems it is often necessary to economize on the representation of the error covariances. This appendix looks at the consequence of neglecting Q_{12}.

Minimising the actual error B^* with $B_{12}^\dagger \equiv 0$ gives:

$$B_{11}^* = \frac{2\sigma_p\sigma_o + a^2}{2a\sigma_o + a^2} \tag{E1}$$

$$B_{12}^* = \frac{Q_{12}}{2\sigma_o + a} \tag{E2}$$

$$B_{22}^* = B_{11}^* - \frac{2c}{s}B_{12}^* + \frac{\sigma_p^2}{s^2}, \tag{E3}$$

where

$$a = \sqrt{\sigma_p^2 + 2\sigma_p\sigma_o} - \sigma_p. \tag{E4}$$

References

Bell, M. J., Martin, M. J. and Nichols, N. K. 2004. Assimilation of data into an ocean model with systematic errors near the equator. *Quart. J. R. Met. Soc.* **130**, 853–871.

Benjamin, S. G., Devenyi, D., Weygandt, S., Brundage, K. J., Brown, J. M. and co-authors 2004. An hourly assimilation-forecast cycle: the RUC. *Mon. Wea. Rev.* **132**, 495–518.

Brogan, W. L. 1991. *Modern Control Theory* 3rd Edition, Prentice Hall, NJ , Englewood Cliffs.

Cohn, S. E., Sivakumaran, N. S. and Todling, R. 1994. A fixed-lag Kalman smoother for retrospective data assimilation. *Mon. Wea. Rev.* **122**, 2838–2867.

Dee, D. P. and Da Silva, A. M. 1998. Data assimilation in the presence of forecast bias. *Quart. J. R. Met. Soc.* **124**, 269–295.

Dee, D. P. and Todling, R. 2000. Data assimilation in the presence of forecast bias: the GEOS moisture analysis. *Mon. Wea. Rev.* **128**, 3268–3282.

Dong, Z. and You, Z. 2006. Finite-horizon robust Kalman filtering for uncertain discrete time-varying systems with uncertain-covarince white noises. *IEEE Sign. Proc. Lett.* **13**(8), 493–496.

Fisher, M., Leutbecher, M. and Kelly, G. A. 2005. On the equivalence between Kalman smoothing and weak-constraint four-dimensional variational data assimilation. *Quart. J. R. Met. Soc.* **131**, 3235–3246.

Gillijns, S. and De Moor, B. 2006. Model error estimation in ensemble data assimilation. *Nonlin. Proc. Geophys.* **14**, 59–71.

Griffin, R. E. and Sage, P. 1969. Sensitivity analysis of discrete filetering and smoothing algorithms. *AIAA J.* **7**, 1890–1897.

Heffes, H. 1966. The effect of erroneous models on the Kalman filter response. *IEEE Trans. Automat. Contr.* **AC-11**, 541–543.

Juckes, M. N. 2006. Evaluation of mipas ozone fields assimilated using a new algorithm constrained by isentropic tracer advection. *Atmos. Chem. Dyn.* **6**, 1549–1565.

Juckes, M. N. 2007. An annual cycle of long lived stratospheric gases from MIPAS. *Atmos. Chem. Dyn.* **7**, 1879–1897.

Juckes, M. N. and Lawrence, B. N. 2006. Data assimilation for re-analyses: potential gains from full use of post-analysis-time observations. *Tellus* **58A**, 171–178, doi:10.1111/j.1600–0870.2006.00167.

Kalman, R. E. and Bucy, R. 1961. New results in linear filtering and prediction. *J. Basic Eng.* **83 D**, 95–108.

Keppenne, C. L., Rienecker, M. M., Kurkowski, N. P. and Adamec, D. D. 2005. Ensemble Kalman filter assimilation of altimeter and temperature data with bias correction and application to seasonal prediction. *Nonlin. Proc. Geophys.* **12**, 491–503.

Li, Z. and Navon, I. M. 2001. Optimality of variational data assimilation and its relationship with the Kalman filter and smoother. *Quart. J. R. Met. Soc.* **127**, 661–684.

Petersen, I. R. and McFarlane, D. C. 1994. Optimal guaranteed cost control and filtering for uncertain linear systems. *IEEE Trans. Autom. Contr.* **39**(9), 1971–1977.

Polavarapu, S., Shepherd, T. G., Rochon, Y. and Ren, S. 2005. Some challenges of middle atmosphere data assimilation. *Quart. J. R. Met. Soc.* **131**, 3513–3527.

Sangsuk-Iam, S. and Bullock, T. E. 1990. Analysis of discrete-time Kalman filtering under incorrect noise covariances. *IEEE Trans. Autom. Contr.* **35**(12), 1304–1309.

Snyder, C. and Zhang, F. 2003. Assimilation of simulated Doppler radar observations with an ensemble Kalman Filter. *Mon. Wea. Rev.* **131**, 1663–1677.

Sørensen, J. V. T., Madsen, H. and Madsen, H. 2006. Parameter sensitivity of three Kalman filter schemes for assimilation of water levels in shelf sea models. *Ocean Modell.* **11**, 441–463.

Stark, H. and Woods, J. W. 2002. *Probability and Random Processes with Applications to Signal Processing* 3rd Edition, Prentice Hall, New Jersey .

Stein, M. L. 1997. Efficiency of linear predictors for periodic processes using an incorrect covariance function. *J. Statist. Plann.* **58**, 321–331.

Todling, R., Cohn, S. E. and Sivakumaran, N. S. 1998. Suboptimal schemes for retrospective data assimilation based on the fixed-lag Kalman smoother. *Mon. Wea. Rev.* **126**, 2274–2286.

Uppala, S. M., Kallberg, P. W., Simmons, A. J., Andrae, U., da Costa Bechtold, V. and co-authors. 2006. The ERA-40 re-analysis. *Quart. J. R. Met. Soc.* **131**, 2961–3012.

Zhang, F., Snyder, C. and Sun, J. 2004. Impacts of initial estimate and observational availability on convective-scale data assimilation with an ensemble Kalman Filter. *Mon. Wea. Rev.* **132**, 1238–1253.

Zhu, Y. Q., Todling, R., Guo, J., Cohn, S. E., Navon, I. M. and co-authors. 2003. The GEOS-3 retrospective data assimilation system: The 6-hour lag case. *Mon. Wea. Rev.* **131**, 2129–2150.